Journal of the Korean Physical Society, Vol. 59, No. 2, August 2011, pp. 1563∼1568

Neutron Resonance Spectroscopy at GELINA

P. Schillebeeckx,* A. Borella, S. Kopecky and C. Lampoudis
EC-JRC, Institute for Reference Materials and Measurements, Retieseweg 111, B-2440 Geel, Belgium

C. Massimi
Department of Physics, University of Bologna and sezione INFN of Bologna, Via Irnerio 46, Bologna, 40126, Italy

M. Moxon
Hyde Copse, Marcham, 3, UK

(Received 26 April 2010)

The neutron time-of-flight facility GELINA installed at the JRC-IRMM Geel (B) has been designed to produce cross section data for neutron induced reactions in the resonance region. It is a multi-user facility, providing a pulsed white neutron source, with a neutron energy range between 10 meV and 20 MeV and a time resolution of 1 ns. The research program concentrates on cross section data needs for nuclear energy applications. In this contribution efforts to improve the quality of cross section data in the resonance region are discussed. These efforts include the implementation of self-indication measurements and improved data reduction and resonance analysis procedures. Due to these efforts accurate neutron-induced cross section data and resonance parameters together with their covariance information can be obtained from thermal up to the unresolved resonance region.

PACS numbers: 28.20.-v, 29.30.-h
Keywords: Neutron cross section data, Transmission, Capture, Time-of-flight, Resonance parameters, Covariance data, REFIT
DOI: 10.3938/jkps.59.1563

I. INTRODUCTION

Neutron induced reaction cross sections are essential data for a wide variety of nuclear applications. Reducing uncertainties of cross section data can lead to significant improvement in the safety assessment and reliability of the predicted performance of new reactor concepts. Most of the data in evaluated data libraries are parameterized by means of nuclear reaction theory. Such a parameterization ensures a consistent description of the total and partial cross sections from the sub-thermal up to the high energy region. In the sub-thermal and resolved resonance region cross sections are described by the R-matrix theory. In the unresolved resonance region, cross sections are based on the Hauser-Feshbach theory including width fluctuations. At higher energies the optical model in addition to statistical and pre-equilibrium reaction theory is used [1].

A resonance is characterized by the energy, spin, parity and the partial widths (neutron $\Gamma_{\rm n}$, radiation Γ_γ, fission $\Gamma_{\rm f}$, ...). The latter express the probability for a specific reaction to occur. Unfortunately no theory exists to predict resonance parameters of individual resonances. Hence, they can only be deduced from experimental data. To determine resonance parameters, a set of complementary independent experimental observables is required [1]. These experimental observables result from transmission, reaction and self-indication measurements [2,3]. The latter are suitable to determine the spin of a resonance [3,4].

In this contribution efforts that have been made at GELINA since the ND2007 conference to reduce bias effects and to produce more accurate cross section data together with their full covariance information are discussed. Issues, such as improved sample characterization procedures [5], the use of self-indication measurements for the determination of the resonance spin [6], and the production of full covariance information [7], are discussed in more detail in other contributions of this conference.

II. GELINA

The time-of-flight (TOF) - facility GELINA has been designed and built for high-resolution cross section measurements in the resolved and unresolved resonance region [8]. It is a multi-user TOF facility, providing a pulsed white neutron source, with a neutron energy range between 10 meV and 20 MeV. The linear electron accelerator produces intense pulses with a width of 10 ns and a nominal peak current of 10 A, at a repetition rate which can range from 10 Hz to 800 Hz. The

*E-mail: peter.schillebeeckx@ec.europa.eu

electrons are accelerated to a maximum energy of 150 MeV. The 10 ns bunches are compressed to less than 1 ns by a post-acceleration compression magnet. These high energy electrons generate Bremsstrahlung in a mercury cooled depleted uranium target, where neutrons are produced by (γ,n) and (γ,f) reactions. The target yields a total neutron intensity of about 3.4×10^{13} s^{-1} when the accelerator is operating at 800 Hz. Two water-filled beryllium containers placed above and below the uranium target, are used as moderators to produce a significant number of neutrons in the low energy region. Using suitable shielding material in the target room, either the direct (fast) neutron spectrum with very good time resolution may be used, or the moderated (slow) neutron spectrum at a reduced resolution. The neutron flux is monitored by 3 BF_3 counters which are mounted in the ceiling of the target hall.

Time-of-flight measurements can be performed simultaneously on 10 flight paths with lengths ranging from 10 m to 400 m. The measurement stations have special equipment, to perform transmission and reaction cross section measurements. Transmission measurements can be performed at 25 m, 50 m, 100 m, 200 m and 400 m. To study the Doppler broadening the station at 25m is equipped with a cryostat to cool the samples down to 10 K. Capture cross section measurements can be carried out at 12.5 m, 30 m, and 60 m using C_6D_6 scintillators. Fission cross section measurements are performed at a 10 m and 30 m station using Frisch gridded ionization chambers and surface barrier detectors. These stations are also used to study (n,p) and (n,α) reactions. Studies of (n,xnγ) reactions are performed at a 30 m and 200 m station using HPGe detectors.

III. NORMALIZATION OF CAPTURE DATA

The stations for capture cross section experiments are equipped with hydrogen-free C_6D_6 detectors. The detectors are placed at 125° with respect to the direction of the incoming neutron beam. This geometry is chosen to minimize systematic effects caused by the anisotropy of dipole radiation. The total energy detection principle in combination with the pulse height weighting technique is applied to make the detection efficiency for a capture event directly proportional to the total γ-ray energy liberated in the capture reaction [9]. For each sample-detection system combination, weighting functions are calculated by Monte Carlo simulations and as much as possible validated by experiment as discussed in Refs. 5 and 9. A procedure to correct for the gamma-ray attenuation in the sample is discussed in Section V. 4. At all measurement stations the incident neutron flux is measured in parallel using either a ^{10}B and/or ^{235}U ionization chamber. The chamber is placed at about 1 m in front of the capture detection system. The ^{10}B(n,α) standard reaction is used to determine the energy dependence of the neutron flux below 150 keV and the ^{235}U(n,f) reaction for energies above 150 keV.

The experimental yield Y_{exp} is deduced from the ratio of the weighted response of the capture detection system and the response of the neutron flux detector:

$$Y_{\rm exp} = N \frac{C_w - B_w}{C_\phi - B_\phi} \, F_\phi \, Y_\phi. \quad (1)$$

This yield is related to the fraction of incident neutrons that interact with the sample and creates a signal in the capture detection system. The dead time corrected weighted response is denoted by C_w and its background contribution by B_w. The dead time corrected TOF-spectrum resulting from the flux measurement is C_ϕ and the background contribution is B_ϕ. The theoretical yield Y_ϕ is given by:

$$Y_\phi = (1 - e^{n_\phi \sigma_{tot}}) \, \frac{\sigma_\phi}{\sigma_{tot}}, \quad (2)$$

where n_ϕ is the areal density of the sensitive layer, ^{10}B or ^{235}U, in the ionization chamber, σ_ϕ is the reference cross section, ^{10}B(n,α) or ^{235}U(n,f), and σ_{tot} is the corresponding total cross section. The factor F_ϕ corrects for the attenuation in the exit window of the ionization chamber and the attenuation due to the air between the chamber and sample.

The time dependent background for a flux measurement is estimated by the black resonance technique [10], *i.e.*, black resonance or notch filters of appropriate thickness are inserted in the beam to remove all neutrons at a given energy. The background as function of TOF is expressed as an analytical function with free parameters that are adjusted to the saturated dips created by notch filters. Most of the capture measurements are executed with at least one notch filter in the beam. The resulting dips in the spectra are used to monitor continuously the background level.

The background contribution for a capture response consists mainly of three components: (1) a time independent component due to ambient radiation and possible radioactivity of the sample; (2) a time dependent component independent of the sample characteristics and (3) a time dependent component that depends on the sample characteristics. The first component is estimated from measurements when the accelerator is not working. The second component is deduced from measurements without a sample in the beam. The third component is due to neutrons and γ-rays scattered by the sample and produce a signal in the detection system. This time dependent component is mainly due to scattered neutrons and depends on the neutron sensitivity of the detection system. The neutron sensitivity of all capture detection systems have been determined by Monte Carlo simulations and verified by experiment [9]. The contribution due to resonance scattering in the sample is included in the resonance shape analysis (RSA) code as explained in [9]. The smooth part of the time-dependent component, mainly due to potential scattering in the sample, was deduced from the response obtained with a ^{208}Pb sample.

This response is normalized based on the macroscopic elastic scattering cross sections and the final contribution is obtained. The adjusted response of the ^{208}Pb sample is verified by the dip resulting from the fixed notch filter(s).

The normalization factor N in Eq. (1) is used to account for the efficiencies and solid angles of the various detectors used in the reaction measurements. This energy independent factor can be determined at a time-of-flight where the theoretical yield is known. Normalization at a known resonance can be performed completely independent of any other cross section for a resonance with $\Gamma_n << \Gamma_\gamma$. In case the macroscopic total cross section is much less than unity ($n\sigma_t << 1$), the capture area is almost proportional to Γ_n and can be determined accurately from independent transmission data. Resonances strong enough to be observed in transmission and used in capture normalization are the 1.15 keV resonance of ^{56}Fe [11] and the 2.25 keV resonance of ^{60}Ni [12]. A normalization independent from any reference cross section can be obtained by normalizing at a saturated resonance [13]. For a saturated resonance the macroscopic cross section is much greater than unity ($n\sigma_t >> 1$) such that nearly all the incident neutrons with energies in the vicinity of the resonance peak interact. In case $\Gamma_n << \Gamma_\gamma$ the yield approaches unity independent of the cross sections.

The normalization of the GELINA capture data are mostly based on an internal saturated resonance. Internal means that the resonance used for normalization is observed within the measurement of the sample/nucleus under study. This often requires the production of special sampless in the form of a mixture or an alloy. When normalizing to an internal resonance all experimental conditions remain unchanged and the impact of various systematic effects is greatly reduced. The use of an internal saturated resonance can result in an uncertainty on the capture yield of below 2%. This has been demonstrated in Ref. 9 where the neutron width for the 1.15 keV resonance of ^{56}Fe has been deduced from measurements with a Fe-Au sandwich sample. The result, $\Gamma_n = 61.3 \pm 1.1$ meV, is in very good agreement with the standard transmission value $\Gamma_n = 61.7 \pm 0.9$ meV by Perey *et al.* [14]. When the normalization is obtained from a resonance of the nucleus under investigation, for certain nuclei also corrections related to the γ-ray emission spectrum are significantly reduced. In the case of ^{232}Th [15], the capture cross section in the URR was deduced by normalizing the data to the yield of the quasi-saturated ^{232}Th resonances at 21.8 eV and at 23.5 eV. A detailed study in [15] of the impact of both the parameters of these resonances and the applied weighting function revealed that the capture cross section in the URR could be determined with an uncertainty of less than 2%.

IV. DATA REDUCTION

To derive the experimental yield or transmission from the TOF-spectra the AGS package is used [7]. This package performs a full propagation of uncertainties, starting from uncorrelated uncertainties due to counting statistics. In addition it uses an elegant approach to separate uncertainties resulting from uncorrelated and correlated components. The uncorrelated part is represented as a diagonal matrix, while the correlated part is expressed as the product of a rectangular matrix with its own transpose. The AGS structure results in a substantial reduction of data storage space and provides a convenient structure to verify the various sources of uncertainties through each step of the reduction process and to study the impact of each component on the final data AGS is routinely used at our institute for data reduction of transmission, capture and fission cross section data Kopecky *et al.* [16] have demonstrated the use of the AGS output to study the different sources of uncertainty on the resonance parameters for the first resonance of ^{113}Cd at 0.178 eV determined from transmission measurements at GELINA.

V. RESONANCE SHAPE ANALYSIS

At GELINA the REFIT [17] code is used to analyze results of cross section experiments and parameterize the data in the resolved resonance region in terms of resonance parameters. The code is based on the Reich-Moore approximation of the R-Matrix formalism and includes modules to account for various experimental effects such as sample in-homogeneities, self-shielding, multiple scattering, Doppler broadening, response of the TOF-spectrometer, neutron sensitivity of the capture detection system and γ-ray attenuation in the sample. The code accommodates numerical and analytical response functions of TOF-facilities. Those for GELINA have been determined by Flaska *et al.* [18] by Monte Carlo simulations. The analytical expressions included in REFIT can be used to describe the results of such simulations.

Resonance parameters are obtained from a least squares adjustment using the expression:

$$\chi^2(t,\vec{a},\vec{b}) = (Z_{\exp}(t) - Z(t,\vec{a},\vec{b}))^T V_Z^{-1} (Z_{\exp}(t) - Z(t,\vec{a},\vec{b})), \quad (3)$$

where t is the time-of-flight, $Z_{exp}(t)$ is the experimental observable and $Z(t,\vec{a},\vec{b})$ the theoretical estimator. The vector $\vec{a}$denotes the input parameters for the reaction model (resonance parameters and scattering radii), while the experimental conditions (*e.g.*, sample characteristics, sample temperature, flight path length, response function) are included in the vector $\vec{b}$. In the general expression of Eq. (3), the matrix V_Z is the covariance matrix of the experimental data. However, in REFIT only the

diagonal term is considered. The theoretical estimate $Z(t, \vec{a}, \vec{b})$ in Eq. (3) is broadened to account for the finite resolution of the TOF-spectrometer:

$$Z(t, \vec{a}, \vec{b}) = \int R(t, \vec{b}, E_n)\; Z'(E_n, \vec{a}, \vec{b})\; dE_n, \qquad (4)$$

where $R(t, \vec{b}, E_n)$ is the response function of the TOF-spectrometer and Z'(E_n) is the theoretical estimate of the experimental observable:

$$Z'(E_n) = \begin{cases} T(E_n) = e^{-n\sigma_{tot}} \\ Y(E_n) = K_c(\sigma_{tot})\; \varepsilon_c(E_n)\; Y_c(E_n) + \\ \qquad\qquad \varepsilon_n(E_n)\; Y_n(E_n) \\ Y_{SI}(E_n) = e^{-n\sigma_{tot}}\; Y(E_n). \end{cases} \qquad (5)$$

The theoretical estimates depend on the nuclear parameters and involve the calculation of Doppler broadened cross sections. They also depend on experimental parameters. The efficiency of the weighted response to detect a capture event or a scattered neutron is denoted by ε_c and ε_n, respectively. Neglecting the internal conversion process, the detection efficiency ε_c of a C_6D_6 detection system is directly proportional to the total excitation energy, which is the sum of the neutron binding energy and the neutron energy in the centre of mass system. This energy dependence is taking into account in REFIT. The efficiency ε_n is the probability that a scattered neutron creates a detectable signal. Equations (3) – (5) reveal that the theoretical yields, $Y(E_n)$ and $Y_{SI}(E_n)$, depend on the experimental conditions and that the correction for neutron sensitivity and γ-ray attenuation can only be done in the RSA. The procedure used to correct for the neutron sensitivity of the detection system, as it is implemented in REFIT, is explained in [9]. The correction for the γ-ray attenuation in the sample, included in the correction factor K_c, is discussed in Section V. 4. In the following, special features of REFIT to treat specific experimental effects are described.

1. Resonance energy

In a TOF-transmission experiment the time difference between the moment that the neutron is created and detected is determined. To deduce the neutron velocity (and the neutron energy), the effective distance L that the neutron has travelled during this time interval is needed. This distance depends on the neutron transport in the target-moderator assembly and the neutron detector or reaction sample. The average path length ΔL the neutron travels within the neutron producing assembly is shown in Fig. 1 as a function of the neutron energy. The results in Fig. 1 are for a GELINA flight path perpendicular to the moderator. The effective flight

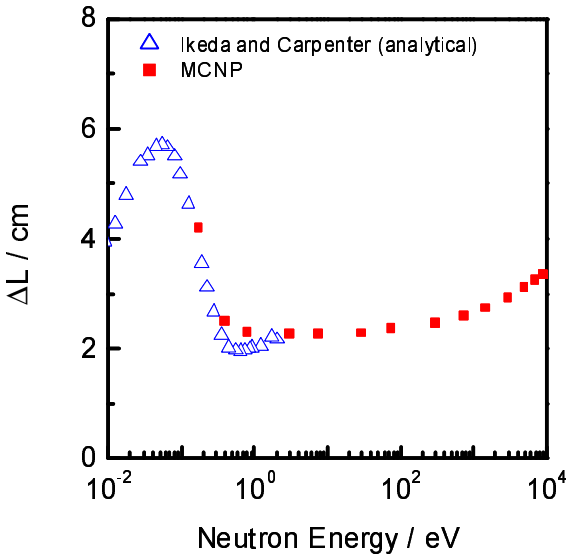

Fig. 1. (Color online) Average distance travelled by the neutron within the target-moderator assembly.

path length L:

$$L(E_n) = L_0 + \Delta L(E_n) \qquad (6)$$

is the sum of ΔL(E_n) and the distance L_0 between the exit face of the moderator and the entrance window of the detector.

Figure 1 reveals that the distance ΔL is a function of the neutron energy. Above 1 eV this distance is approximately half the thickness of the moderator. The strong energy dependency below 1 eV is due to the storage term introduced by Ikeda and Carpenter [19]. In REFIT an analytical expression for this storage term is implemented. Since ΔL depends on the response function of the TOF-spectrometer used in the analysis, a metric measurement of L_0 is not sufficient to define L. The flight path length of every transmission station is calibrated using the 6.6735 $\pm$ eV resonance of ^{238}U+n as a reference. This energy results from transmission measurements performed at ORELA [20]. By combining systematically transmission and reaction cross section data in the RSA, the energy of all resonances, also of those which are not observed in transmission, are traceable to the 6.6735 eV resonance of ^{238}U. For a correct RSA it is of primary importance that the data in the EXFOR library are reported as a function of TOF and that the response function of the spectrometer is specified, as recommended in [7].

2. Sample inhomogeneities

In Ref. 21 the influence of the variation in the areal density, caused by, *e.g.*, the particle size in thin powder samples, has been discussed. A method to study this effect and to describe the variation in the areal density was presented. This method was based on Monte

Carlo simulations and an analytical approach. The analytical approach, using a log-normal distribution of the areal density, has been implemented in REFIT. A RSA of transmission data obtained at GELINA on $^{240}PuO_2$ and $^{242}PuO_2$ oxide powder mixed with graphite was performed. The results revealed that ignoring sample inhomogeneities in the analysis leads to an overestimation of the total width and an underestimation of the peak cross section, with errors reaching between 10% and 30%. Although even using REFIT such bias effects can be avoided, the use of solutions (either in the form of very low enriched materials or as sol-gel based samples, as in Ref. 22) is definitely recommended.

3. Capture events after neutron scattering

In capture cross section measurements the observed capture yield is a sum of the contribution of neutrons that are captured without having suffered any prior scattering interaction and of neutrons that are captured in the sample after at least one neutron scattering interaction. In REFIT there are two options that can be used to account for scattering plus capture events in the sample: a full and a simple Doppler broadening option. In the full option the nuclear cross sections in the laboratory system are Doppler broadened and the thermal motion of the sample nuclei is taken into account in the calculation of the energy of the scattered neutron. In the simple option this effect is not taken into account. For the mathematical implementation reference is made to the REFIT [17] and SAMMY [23] manual. It should be noted that the procedure used in SAMMY for scattering corrections is based on the simple option in REFIT.

In Figs. 2 and 3 the experimental yield around the 69 eV resonance of ^{232}Th is shown. The data result from a capture measurement at GELINA on a 1 mm thick and 80 mm diameter ^{232}Th disk. The experimental data are compared with the result of calculations with SAMMY and the result using the full option in REFIT. Figure 3 shows that in the peak region the full Doppler broadening option of REFIT is needed to describe the experimental data. In Figs. 2 and 3 the different contributions are also shown: Y_0 is the self-shielded capture yield, Y_1 is the capture yield after only one neutron scattering and Y_2 represents the capture yield after at least two neutron scatterings. The results in Fig. 2 indicate that the contribution of the Y_2 term for the 69 eV resonance is negligible.

Figure 4 shows the result from a capture measurement at GELINA on a 3-mm thick Mn sample. This figure illustrates that in case the Y_2 term dominates the observed yield the agreement is not good and also the model in REFIT partly fails. These discrepancies and possible improvements to REFIT are under investigation.

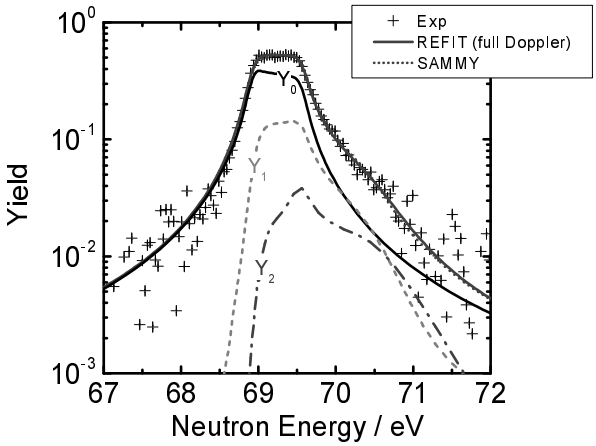

Fig. 2. Comparison of the experimental and calculated yield around the 69 eV resonance of ^{232}Th.

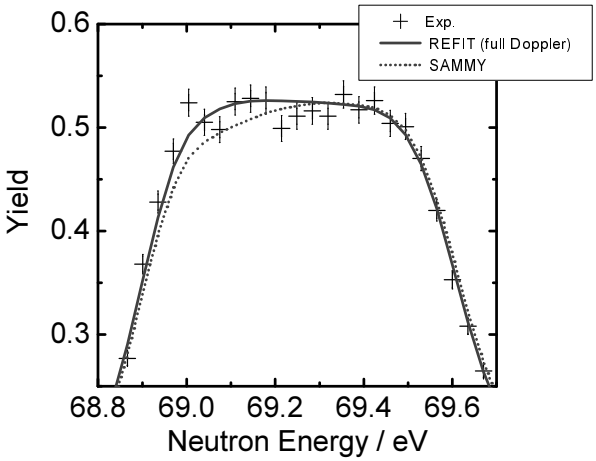

Fig. 3. Comparison of the experimental and calculated yield in the peak region of the 69 eV resonance of ^{232}Th.

4. Gamma-ray attenuation in the sample

The various contributions Y_i to the observed yield, as defined in the previous section, will have a different spatial distribution in the sample. Therefore, the attenuation of γ-rays emitted after a neutron has been captured, will be different for each of these contributions. To account for this effect the procedure proposed in [9] has been implemented in REFIT. In this approach the weighting functions are applied for a homogeneous distribution of the γ-rays in the sample and a correction factor $K_{c,i}$ for each contribution Y_i is used in Eq. (5).

The importance to account for the gamma-ray attenuation effect is illustrated in Fig. 5. This figure compares the yield observed for a 0.5-mm thick ^{197}Au sample with a theoretical yield obtained for a homogeneous distribution of all γ-rays in the sample and a yield obtained by supposing a different γ-ray attenuation correction for each contribution Y_i. In the two cases the experimental data have been normalized in the region of the saturated

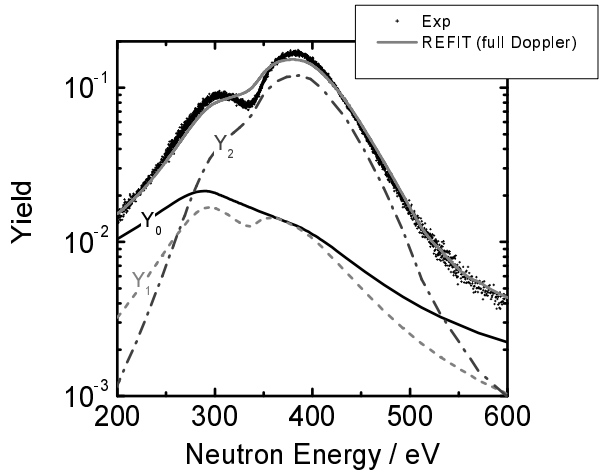

Fig. 4. Comparison of the experimental and calculated yield for ^{55}Mn obtained with a 3-mm thick sputtering sample.

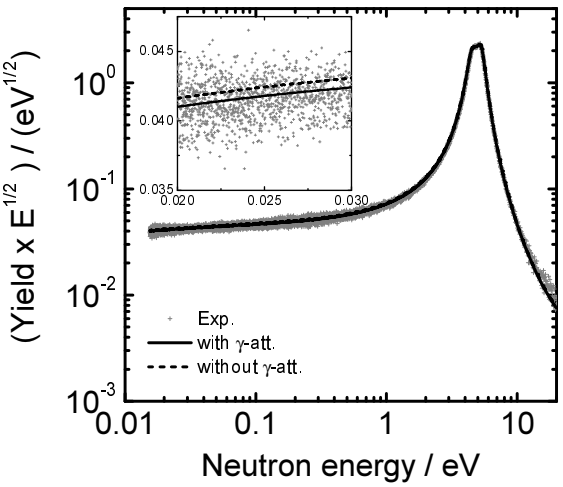

Fig. 5. Capture yield (multiplied by the $E^{1/2}$) as a function of energy for a 0.5-thcik Au-sample at 12.5 m.

resonance. The theoretical yield is calculated using the resonance parameters in ENDF/B-VII [24]. The parameters in this file have been adjusted to reproduce a thermal capture reaction of 98.7 b, which is considered as a standard [25]. Only by correcting for the γ-ray attenuation the yield in the thermal region can be reproduced. Without this correction the calculated curve deviates by 1.5% from the observed yield (see Fig. 5).

VI. SUMMARY

Experimental effects (*i.e.*, response function of the TOF-spectrometer, sample characteristics, scattering corrections, γ-ray attenuation) affecting the data in the resonance region have been discussed. These effects must be considered in the RSA to avoid bias effects and produce accurate data and resonance parameters with reliable covariance information. The implementation of these effects in REFIT is part of an ongoing effort at our institute to improve the quality of cross section data in the resonance region.

ACKNOWLEDGMENTS

The work was supported by the European Commission within the Sixth Framework Programme through EFNUDAT (EURATOM contract no. FP6-036434)

REFERENCES

[1] F. H. Fröhner, JEFF Report 18, NEA/OECD, 2000.
[2] F. Rahn *et al.*, Phys. Rev. C: Nucl. Phys. **6**, 1854 (1972).
[3] J. E. Lynn, F. W. K. Firk and M. C. Moxon, Nucl. Phys. **5**, 603 (1958).
[4] C. Massimi *et al.*, Nuovo Cimento. **125** (2010).
[5] C. Lampoudis *et al.*, *Inter. Conf. on Nucl. Data for Sci. and Techn.-ND2010* (Jeju, Korea, 2010).
[6] C. Massimi *et al.*, *Inter. Conf. on Nucl. Data for Sci. and Techn.-ND2010* (Jeju, Korea, 2010).
[7] N. Otuka *et al.*, *Inter. Conf. on Nucl. Data for Sci. and Techn.-ND2010* (Jeju, Korea, 2010).
[8] D. Tronc, J. M. Salomé and K. H. Böckhoff, Nucl. Instrum. Methods **228**, 217 (1985).
[9] A. Borella *et al.*, Nucl. Instrum. Methods Phys. Res. Sect. A **577**, 626 (2007).
[10] D. B. Syme, Nucl. Instrum. Methods **198**, 357 (1982).
[11] A. Borella *et al.*, Phys. Rev. C: Nucl. Phys. **76**, 014605 (2007).
[12] F. Corvi *et al.*, Nucl. Phys. A **697**, 581 (2002).
[13] R. L. Macklin, J. Halperin and R. R. Winters, Nucl. Instrum. Methods **164**, 213 (1979).
[14] F. G. Perey, in *Proceedings of Inter. Conf. on Nuclear Data for Basic and Applied Science* (Santa Fe, US, 1985), p. 1523.
[15] A. Borella *et al.*, Nucl. Sci. Eng. **152**, 1 (2006).
[16] S. Kopecky *et al.*, Nucl. Instrum. Methods Phys. Res. Sect. B **267**, 2345 (2009).
[17] M. C. Moxon and J. B. Brisland, AEA-InTec-0630, AEA Technology, 1991.
[18] M. Flaska *et al.*, Nucl. Instrum. Methods Phys. Res. Sect. A **531**, 394 (2004).
[19] S. Ikeda and J. M. Carpenter, Nucl. Instrum. Methods Phys. Res. Sect. A **239**, 536 (1985).
[20] H. Derrien *et al.*, ORNL/TM-2005/241, Oak Ridge National Laboratory, 2005.
[21] S. Kopecky, P. Siegler and A. Moens, in *Proceedings of Inter. Conf. on Nucl. Data for Sci. and Techn.* (Nice, France, 2007), p. 623.
[22] N. M. Larson, ORNL/TM-9179/R8, Oak Ridge National Laboratory, 2008.
[23] C. Lampoudis *et al.*, *Inter. Conf. on Nucl. Data for Sci. and Techn.-ND2010* (Jeju, Korea, 2010).
[24] M. B. Chadwick *et al.*, Nucl. Data Sheets **107**, 2931 (2006).
[25] A. D. Carlson *et al.*, Nucl. Data Sheets **110**, 3215 (2009).